Physica C 491 (2013) 24–29

Contents lists available at SciVerse ScienceDirect

Physica C

journal homepage: www.elsevier.com/locate/physc

Synchronization of Josephson oscillations in a mesa array of $Bi_2Sr_2CaCu_2O_{8+\delta}$ through the Josephson plasma waves in the base crystal

Shi-Zeng Lin [a,*], Alexei E. Koshelev [b]

[a] Theoretical Division, Los Alamos National Laboratory, Los Alamos, NM 87545, USA
[b] Materials Science Division, Argonne National Laboratory, Argonne, IL 60439, USA

ARTICLE INFO

Article history:
Accepted 20 November 2012
Available online 29 November 2012

Keywords:
Intrinsic Josephson junctions
Terahertz radiation
Synchronization
Mesa array

ABSTRACT

Using mesa array fabricated at the top of $Bi_2Sr_2CaCu_2O_8$ single crystal was demonstrated recently as a promising route to enhance the radiation power generated by the Josephson oscillations in mesas. We study the synchronization in such an array via the plasma waves in the base crystal. First, we analyze plasma oscillations inside the base crystal generated by the synchronized mesa array and the associated dissipation. We then solve the dynamic equation for the superconducting phase numerically to find conditions for synchronization and to check the stability of the synchronized state. We find that the mesas are synchronized when the cavity resonance of mesas matches with that of the base crystal. An optimal configuration of the mesa arrays is also obtained.

© 2012 Elsevier B.V. All rights reserved.

1. Introduction

Soon after the discovery of Josephson Effects, it was realized that Josephson junction can be used to generate electromagnetic waves. When the junction is biased in voltage state with voltage V, the two superconducting electrodes have energy difference 2 eV. The system is similar to two-energy level system in atomic physics. When Cooper pairs tunnel from the electrode with higher energy to that with lower energy, a photon with angular frequency $\omega = 2\,\mathrm{eV}/\hbar$is emitted. The frequency can be tuned by voltage and 1 mV corresponds to 0.483 THz. The radiation power from one junction however is weak, of the order of 1 pW [1–3]. Arrays of Josephson junctions are fabricated to enhance the radiation power [4–8]. Once these junctions are synchronized, the total radiation power is proportional to the number of junctions squared.

A stack of Josephson junctions is naturally realized in some layered cuprate superconductor [9], such as $Bi_2Sr_2CaCu_2O_{8+\delta}$ (BSCCO). Because of the large superconducting energy gap (up to 60 meV), these build-in intrinsic Josephson junctions (IJJs) may have Josephson oscillations with frequencies in the terahertz (THz) band. IJJs are packed on nanometer scale, much smaller than the THz electromagnetic (EM) wavelength, and are homogeneous. The THz generator based on IJJs thus is promising to fill the THz gap [10,11]. Many efforts have been made in the last decade to excite the coherent THz radiation experimentally [12–15]. On the theoretical side, numerical simulations and analytical calculations have been performed to understand the mechanism of radiation [16–26].

Coherent radiation from a mesa structure of BSCCO in the absence of external magnetic fields was observed experimentally in 2007 [27], which renewed the interest in this field. It was found that the mesa itself forms a cavity to synchronize the radiation in different layers, as evidenced from the dependence of the radiation frequency f on the lateral size L of the mesa, $f = c_0/(2L)$ with $c_0 = c/\sqrt{\epsilon_c}$ the Josephson plasma velocity where ϵ_c is the dielectric constant of BSCCO. The cavity resonance mechanism has been confirmed by many independent experiments [28–32] and the radiation power is enhanced to about 30 μW [33]. A dynamic state with the π phase kink was proposed to account for the experimental observations [34,35]. It was suggested that the strong in-plane dissipation is responsible for the c-axis uniform excitation of the cavity mode [36].

From application perspective, the radiation power in the present experimental design is still too weak to be practically useful. A natural way to enhance the radiation power by using thicker mesas has several challenges. First, for a thick mesa it becomes difficult to cool the system efficiently. The dissipation and hence self-heating increase with the volume of the mesa, while the heat removal rate remains the same because the heat is mainly removed through the substrate. It has already shown experimentally that even for a mesa with thickness of ~2 μm, central part of the mesa is driven to the normal state by the severe self-heating [29,30]. Secondly, it was calculated that for a tall mesa a long-range instability destroying the in-phase plasma oscillations develops [37], and only parts of the mesa can be synchronized [36].

To enhance the radiation power while minimizing the self-heating, one may use multiple thin mesas on top of the same BSCCO single crystal. The multiple mesa structures have been fabricated

* Corresponding author.
E-mail addresses: szl@lanl.gov (S.-Z. Lin), koshelev@anl.gov (A.E. Koshelev).

0921-4534/$ - see front matter © 2012 Elsevier B.V. All rights reserved.
http://dx.doi.org/10.1016/j.physc.2012.11.008

recently and it was demonstrated that the radiation power is enhanced under appropriate conditions [38,39]. The mechanism of synchronization among mesas is not known. There are two sources of interaction. The mesas interact through the radiation fields. They also interact through the plasma oscillations excited in the base crystal. The resonance damping due to the leaking of radiation from the mesa into the base crystal has been considered in Ref. [40] and it was demonstrated that this channel gives the main contribution to the dissipation. Therefore, synchronization mediated by the radiation fields inside the crystal is probably a dominating mechanism. The present work is devoted to understanding the synchronization of multiple mesas through the plasma oscillations in the base crystal and to finding an optimal configuration for synchronization.

2. Model

We consider arrays of identical mesas with the period a atop of a BSCCO single crystal as schematically shown in Fig. 1. Every mesa contains N_m junctions and has width L while the base crystal contains N_c junctions. No external magnetic field is applied. Each mesa is biased independently by a *dc* current injected from the top of the mesa and extracted from the top surface of crystal. In this case, the junctions in the basal crystal remain in the zero-voltage state, and the mesas are driven into resistive state. The system is assumed to be uniform along the y direction and the problem becomes two dimensional. The dynamics of the gauge-invariant phase difference θ_n and magnetic field h_n in the n-th junction are described by [41–45]

$$\frac{\partial^2\theta_n}{\partial\tau^2} + v_c\frac{\partial\theta_n}{\partial\tau} + \sin\theta_n - \ell^2\frac{\partial h_n}{\partial x} = 0 \tag{1}$$

$$\left(\ell^2\nabla_n^2 - 1\right)h_n + \frac{\partial\theta_n}{\partial x} + v_{ab}\frac{\partial}{\partial\tau}\left(\frac{\partial\theta_n}{\partial x} - h_n\right) = 0 \tag{2}$$

where $\nabla_n^2 f_n \equiv f_{n+1} + f_{n-1} - 2f_n$ is the finite difference operator. Here the time and coordinate are measured in units of the inverse Josephson plasma frequency $1/\omega_p$ and the Josephson length $\lambda_J = \gamma s$ correspondingly and the unit of magnetic field is $\Phi_0/(2\pi\gamma s^2)$, where γ is the anisotropy factor and s is the interlayer spacing. Here $\omega_p = c/(\lambda_c\sqrt{\epsilon_c})$ and $\Phi_0 = hc/(2e)$ is the flux quantum. These reduced equations depend on three parameters, $v_c = 4\pi\sigma_c/(\varepsilon_c\omega_p)$, $v_{ab} = 4\pi\sigma_{ab}/(\varepsilon_c\omega_p\gamma^2)$, and $\ell = \lambda_{ab}/s$, where σ_c and σ_{ab} are the quasiparticle conductivity, and λ_c and λ_{ab} are the London penetration depth along the c-axis and ab-plane respectively. The dimensionless electric field in units of $\Phi_0\omega_p/(2\pi cs)$ is given by $E_{z,n} = \partial_t\theta_n$.

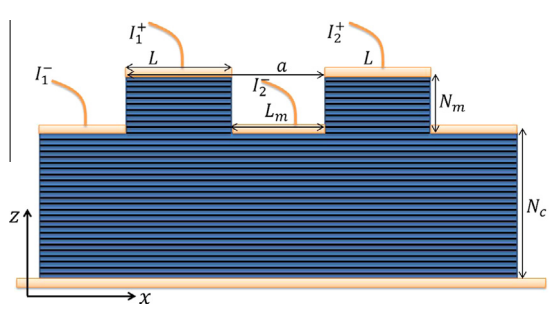

Fig. 1. Schematic view of multiple mesas atop of a BSCCO crystal. The mesas are biased independently. The BSCCO sample (blue) is sandwiched by gold electrodes (orange). *In the analytical treatment*, we consider an array of identical mesas with width L and period a. The top surface of the base crystal is free. *In the simulation part*, we consider two identical mesas with width L separated by a distance L_m. The mesas are located at the position L away from the edges of the base crystal. The top surface of the base crystal is also covered by gold electrodes through which the current is extracted. (For interpretation of the references to color in this figure legend, the reader is referred to the web version of this article.)

For the mesa with thickness of 1 μm which is much smaller than the wave length of THz EM wave in vacuum, there is a significant impedance mismatch between the mesa and vacuum [46]. Most part of energy is reflected at the edges of mesa and cavity resonance is achieved. We can use the boundary condition that the oscillating magnetic field vanishes at the edges. The boundary condition at the edges of the mesas is $\partial_x\theta_n = \pm L\, I_\mu/2$, and the boundary condition at the edges of the base crystal is $\partial_x\,\theta_n = 0$, where I_μ is the bias current in the μ-th mesa. We assume that the contact material can be approximated by an ideal conductor so that the tangential oscillating current vanishes at the conductor surface corresponding to the boundary condition $\partial_z h(z) = 0$ in the continuum limit.

3. Plasma oscillations excited in the base crystal in the synchronized state

In this section, we calculate the plasma oscillations in the synchronized state assuming that the array contains large number of mesas so that it can be treated as an infinite system. The time dependence of the phases in mesas in resistive state has the form $\theta_n(x,t) = \omega\tau + \varphi_n(x) + \mathrm{Re}[\theta_n(x)\ \exp\ (-i\omega\tau)] + \psi_\mu$ and in the crystal the phases have only have small oscillations. Here ψ_μ account for the possible phase shifts between the synchronized mesas. We consider the case with $\psi_\mu = 0$ and leave a more general case for the numerical simulation in the next Section. We consider voltage range corresponding to the Josephson frequencies close to the fundamental cavity resonance $\omega \approx \omega_1 = \ell\pi/L$. For definiteness, we assume that in the mesas the kink state is formed [34,35] providing strong coupling to the cavity resonance meaning that we can use approximations $\varphi_n\ (x) \approx \pi[\mathrm{sgn}(x)+1]/2$ and $\sin\theta_n = -\mathrm{Re}[i\exp\ (-i\omega\tau - i\varphi_n(x))] \approx g(x)\mathrm{Re}[i\exp\ (-i\omega\tau)]$ with $g(x) \approx \mathrm{sgn}(x)$. However, a particular shape of the modulation function $g(x)$ has no importance in further derivations. For an isolated mesa on the top of bulk crystal this problem was considered in Ref. [40] where it was concluded that leaking radiation into the crystal provides dominating mechanism of resonance damping.

The amplitudes of the phases and magnetic fields obey the following equations: in mesas for $|x - ma| < L/2$, $0 < n < N_m$,

$$(\omega^2 + iv_c\omega)\theta_n + \ell^2\frac{\partial h_n}{\partial x} = ig(x) \tag{3}$$

$$\ell^2\nabla_n^2 h_n - (1 - iv_{ab}\omega)h_n + (1 - iv_{ab}\omega)\frac{\partial\theta_n}{\partial x} = 0 \tag{4}$$

and in the crystal, for $-N_c < n \leqslant 0$, the first equation has to be modified as

$$(\omega^2 - 1 + iv_c\omega)\theta_n + \ell^2\frac{\partial h_n}{\partial x} = 0. \tag{5}$$

Using the presentation $g(x) = \sum_{m=0}^{\infty} g_m \sin(p_m x)$ with $p_m = (2m-1)\pi/L$, we can find solution of these equations as mode expansions. In particular, the oscillating magnetic field in the mesas can be written as

$$h_n^{(\mathrm{m})}(x) = \sum_{m=1}^{\infty}\frac{ip_m(g_m + a_m\cos[q_m(n - N_\mathrm{m} - 1/2)])}{\omega^2 + iv_c\omega - \ell^2 p_m^2}\cos(p_m x),$$

for $n > 0$, where $q_m \equiv q(p_m,\omega)$ with $\mathrm{Im}(q_m) > 0$ is the wave vector describing propagation of the plasma wave along c-axis for the fixed in-plane wave vector and frequency,

$$\cos q_m = 1 + \frac{1 - iv_{ab}\omega}{2\ell^2}\left(1 - \frac{\ell^2 p_m^2}{\omega^2 + iv_c\omega}\right). \tag{6}$$

In the crystal, $n \leqslant 0$, the oscillating magnetic field can be presented as Fourier series,

$$h_n^{(\mathrm{cr})}(x) = \frac{1}{a}\sum_{k=2\pi l/a} H_k \cos[q_k(n+N_c+1/2)]\exp(ikx) \tag{7}$$

with

$$\cos q_k = 1 + \frac{1-i\nu_{ab}\omega}{2\ell^2}\left(1-\frac{\ell^2k^2}{\omega^2-1+i\nu_c\omega}\right).$$

It is crucial that the synchronized mesa array excites discrete set of modes inside the crystal. For the fixed k, the frequency range $\omega^2 < 1+\ell^2k^2$ corresponds to propagating waves along the c-axis while the range $\omega^2 > 1+\ell^2k^2$ corresponds to evanescent waves. At the frequency $\omega^2 = 1+\ell^2k^2$ the uniform plasma mode is excited. The decay length of the plasma mode in terms of the number of junctions, $N_d(\omega) = 1/\mathrm{Im}[q_k(\omega)]$, has a sharp maximum at this frequency, see Fig. 2. For $a \approx 2L$ the mode with the wave vector $k = 2\pi/a$ plays the most important role, because the frequency of the uniform mode $\omega = \sqrt{1+\ell^2(2\pi/a)^2}$ is close to the cavity-resonance frequency inside the mesa $\omega_1 = \ell\pi/L$.

The unknown coefficients a_m and H_k have to be found from matching at the interface, $h_n^{(\mathrm{m})}(x) = h_n^{(\mathrm{cr})}(x)$ for $n = 0,1$. Taking the projection of the equation $h_0^{(\mathrm{m})}(x) = h_0^{(\mathrm{cr})}(x)$ to mode m, using

$$S_m(k) = \int_{-L/2}^{L/2} dx\cos(p_m x)\cos kx = \frac{2(-1)^m p_m\cos[kL/2]}{p_m^2-k^2},$$

we obtain equation expressing a_m via H_k

$$\frac{ip_m(g_m + a_m\cos[q_m(N_\mathrm{m}+1/2)])}{\omega^2+i\nu_c\omega-\ell^2p_m^2} = \frac{1}{a}\sum_{k=2\pi l/a} H_k\cos[q_k(N_c+1/2)]\frac{4(-1)^m}{L}\frac{p_m\cos[kL/2]}{p_m^2-k^2}.$$

Note that $S_m(k)$ satisfy the orthogonality conditions

$$\frac{2}{aL}\sum_{k=2\pi l/a} S_m(k)S_{m'}(k) = \delta_{mm'}.$$

On the other hand, the inverse Fourier transform of the equation $h_1^{(\mathrm{m})}(x) = h_1^{(\mathrm{cr})}(x)$ allows us to express H_k via a_m

$$H_k\cos[q_k(N_c+3/2)] = \sum_{m=1}^{\infty}\frac{2(-1)^m ip_m^2}{\omega^2+i\nu_c\omega-\ell^2p_m^2} \times \frac{\cos[kL/2]}{p_m^2-k^2}(g_m + a_m\cos[q_{m'}(N_\mathrm{m}-1/2)]).$$

Eliminating H_k, we obtain the linear equations for a_m

$$(\cos[q_m(N_\mathrm{m}-1/2)] - \cos[q_m(N_\mathrm{m}+1/2)])a_m - \sum_{m'=1}^{\infty}\mathcal{J}_{mm'}a_{m'}\cos[q_{m'}(N_\mathrm{m}-1/2)] = \sum_{m'=1}^{\infty}\mathcal{J}_{mm'}g_{m'}$$

with the matrix

$$\mathcal{J}_{mm'} = \frac{p_{m'}(\omega^2+i\nu_c\omega-\ell^2p_m^2)}{p_m(\omega^2+i\nu_c\omega-\ell^2p_{m'}^2)}\frac{2}{aL} \times \sum_{k=2\pi l/a} S_m(k)S_{m'}(k)\left(1-\frac{\cos[q_k(N_c+1/2)]}{\cos[q_k(N_c+3/2)]}\right).$$

Near the fundamental-mode resonance $\omega \approx \ell p_1$ the amplitude a_1 dominates and we can use the single-mode approximation neglecting all other amplitudes. This leads to the simple result

$$a_1 \approx \frac{g_1\mathcal{J}_{11}}{\cos[q_1(N_\mathrm{m}-1/2)] - (1+\mathcal{J}_{11})\cos[q_1(N_\mathrm{m}+1/2)]} \approx \frac{g_1\mathcal{J}_{11}}{q_1\sin[q_1N_\mathrm{m}] - \mathcal{J}_{11}\cos[q_1(N_\mathrm{m}+1/2)]} \tag{8}$$

with

$$\mathcal{J}_{11} = \frac{2}{aL}\sum_{k=2\pi l/a}\frac{4p_1^2\cos^2[kL/2]}{(p_1^2-k^2)^2}\left(1-\frac{\cos[q_k(N_c+1/2)]}{\cos[q_k(N_c+3/2)]}\right)$$

and $q_1 \approx \sqrt{-\frac{1-i\nu_{ab}\omega}{\ell^2}\frac{\omega^2-\ell^2p_1^2+i\nu_c\omega}{\omega^2+i\nu_c\omega}}$. With this result, one can obtain the oscillating phases and fields in the mesa. Also using Eq. (3) and keeping only $m = 1$ in the sum, we obtain the coefficients H_k which determine the oscillating magnetic field inside the crystal, Eq. (7). For an isolated mesa on bulk crystal corresponding to the limit $a, N_c \to +\infty$, the following approximate result can be derived [40] $\mathcal{J}_{11} \approx \sqrt{1-i\nu_{ab}\omega}(0.57+0.31i)/\ell$, suggesting the following presentation $\mathcal{J}_{11} = \sqrt{1-i\nu_{ab}\omega}\beta_1/\ell$, where β_1 is the complex function of the order unity. The amplitude of the oscillating magnetic field on the top of the mesa can be represented as

$$h_{N_\mathrm{m}}^{(\mathrm{m})}(x) \approx \frac{ip_1g_1\cos(p_1x)}{\omega^2-\ell^2p_1^2+i\nu_c\omega+\mathcal{A}_1(\omega)}, \tag{9}$$

where the complex function $\mathcal{A}_1(\omega)$

$$\mathcal{A}_1 = -\frac{(\omega^2-\ell^2p_1^2+i\nu_c\omega)\beta_1}{\sqrt{-\frac{\omega^2-\ell^2p_1^2+i\nu_c\omega}{\omega^2+i\nu_c\omega}}\sin[q_1N_\mathrm{m}] + \beta_1\left(1-\cos\left[q_1\left(N_\mathrm{m}-\frac{1}{2}\right)\right]\right)}$$

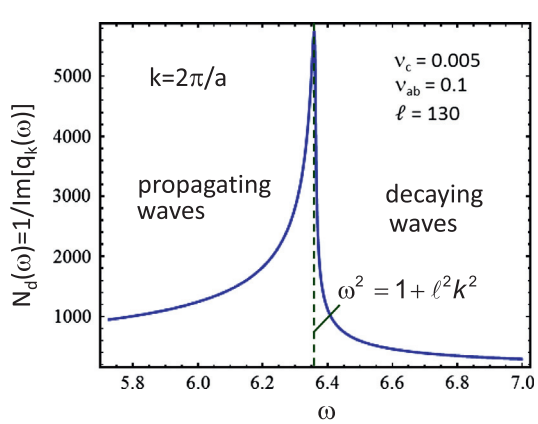

Fig. 2. The frequency dependence of the decay length along c-direction, N_d, for the fixed in-plane wave vector and representative parameters specified in the plot.

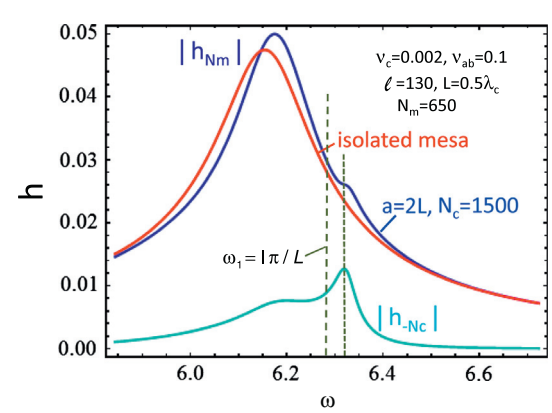

Fig. 3. Comparison of the frequency dependence of the oscillating magnetic field at the mesa top for isolated mesa and mesa array. The frequency dependence of the oscillating magnetic field at the bottom of the base crystal for mesa array is also shown. Parameters used in calculations are specified in the plot.

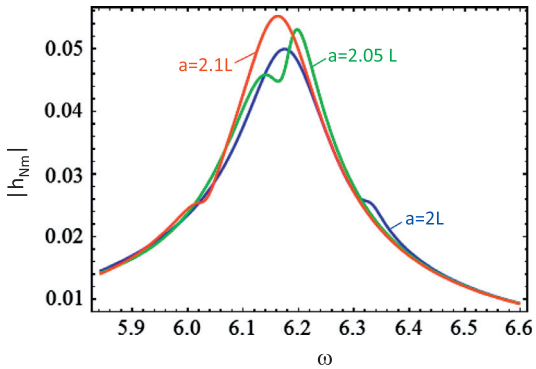

Fig. 4. The frequency dependences of the oscillating magnetic field at the mesa top for different periods of the mesa array. Other parameters are the same as in the previous plot.

determines the damping of the resonance and its frequency shift in all quantities.

Fig. 3 illustrates the Josephson-frequency dependence of the oscillating magnetic field amplitude inside the mesa near the cavity-resonance frequency for the isolated mesa and for the mesa array with $a = 2L$. One can see that for used parameters the corrections are weak. Above the main peak one can see a small dip caused to excitation of the almost uniform standing wave inside the crystal. To verify this, we also show the plot of the oscillating magnetic field at the bottom of the base crystal. The dip in the mesa field corresponds to the rather sharp peak of the field at the bottom of the crystal. Note also that the resonance is displaced to lower frequency with respect to the uniform cavity mode $\ell\pi/L$ because plasma oscillations excited inside the mesa are not uniform in the c direction. The width of resonance is mostly determined by the leak of radiation into the base crystal. The dip is located slightly below the frequency of the uniform plasma wave inside the crystal which for these parameters is larger than the cavity-resonance frequency.

Fig. 4 shows evolution of the resonance shape with variation of the array period a. We can see that with increasing a the dip moves to smaller frequencies. The dip has maximum amplitude and located at the peak for $a = 2.05L$. It is interesting to note that the resonance in mesa is actually strongest when the dip is located *below* the peak at $a = 2.1L$. The reason is that in this case the wave excited at the peak frequency and the wave vector $k = 2\pi/a$ is in decaying range, see Fig. 2 and, as consequence, the mesas loose less energy to radiation at the resonance frequency. Nevertheless, we expect the strongest interaction between the mesas and optimal conditions for synchronization when the two resonances coincide.

4. Numerical Simulations

To find the condition for synchronization between mesas and checked the stability of the synchronized state, we solve Eqs. (1) and (2) numerically for two mesas. The details of the numerical procedure are presented in Ref. [36]. The number of junctions in the base is $N_c = 200$ and in the mesa is $N_m = 50$. We take $\nu_c = 0.02$, $\nu_{ab} = 0.2$ and $\ell = 266.5$. To ensure that the resulting state is stable, we add an artificial weak white noise current in Eq. (1) in simulations, $\langle \widetilde{I}_n(x,t)\widetilde{I}_{n'}(x',t')\rangle = 10^{-5}\delta(x-x')\delta(t-t')\delta(n-n')$. To study the coherence between the different stacks, we introduce the order parameters at the mesas' edges

$$r_{\mu,L/R} = \frac{1}{N_m}\sum_{n}^{N_m}\exp(i\theta^{\mu}_{n,L/R}), \tag{10}$$

where $\theta^{\mu}_{n,L/R}$ is the phase difference for n-th junction at the left (L) or right (R) edge of the μ-th mesa. The time average of $|r_{\mu,L/R}|, \bar{r}_{\mu,L/R} = \int_0^T |r_{\mu,L/R}|dt/T$ measures the phase coherence at the edges of the mesa. For coherent oscillations of phase difference $r_{\mu,L/R} = 1$ and for completely random oscillations $r_{\mu,L/R} \to 0$ when $N_m \to \infty$. To quantify the phase coherence between different mesas, we introduce a correlation function

$$g_{\mu,L/R} = \frac{1}{T}\int_0^T r^*_{1,L} r_{\mu,L/R}dt, \tag{11}$$

where we have taken the left edge of the first mesa as a reference. The amplitude $|g_{\mu,L/R}|$ measures the coherence between the phase oscillations at left or right edges of the μ-th mesa and at the left edge of the first mesa while the phase of $g_{\mu,L/R}$ represents the phase shift between them.

Let us first consider two identical mesas with width $L = 0.3\lambda_c$ and with a separation L_m. They locate at the position L away from the edges of the base crystal. They are biased by the same current, $I_1 = I_2 = I_{ext}$, as shown in Fig. 6a. The results for different L_m is shown in Fig. 5. The main peak at the left side corresponds to the fundamental cavity mode of the mesa $\omega_1 = \ell\pi/L$ and the the peak at the right side corresponds to the second cavity mode $\omega_2 = 2\ell\pi/L$. When the frequency of the plasma oscillations in the mesa matches the cavity frequencies $\omega_m = m\ell\pi/L$, $|g_{j,L/R}|$ increases indicating a tendency of synchronization between the two stacks. When $L_m \approx nL$, the phase coherence between the different mesas becomes maximal. This is clearer for the second cavity mode, where the two stacks do not synchronize at all when $L_m \neq nL$. For $L_m = 0.7\lambda_c$, the peak at $I_{ext} = 2.0I_c$ is due to the cavity resonance inside the mesa. However the resonance occurs at smaller I_{ext} compared to that with $L_m = nL$. The downshift is due to the strong radiation damping through the base crystal as shown in Fig. 3.

The reasons for the better coherence when $L_m = nL$ are as follows. For the plasma oscillations uniform along the c axis with $q_k = 0$, the in-plane dissipation is absent and the plasma mode is only damped by the weak dissipation along the c-axis according to Eq. (6). However, for nonuniform oscillations with a finite wavenumber q_k, the in-plane dissipation becomes dominant for $N_m \lesssim 10^3$, and the nonuniform plasma oscillations in the base crystal decays quickly. Therefore the interaction between two mesas is weak and the synchronization becomes difficult. When $L_m = nL$, the uniform cavity modes with $q_k = 0$ are efficiently excited as shown in Fig. 6a and b. In this case two mesas are strongly coupled through the base crystal and they can be easily synchronized. When $L_m \neq nL$, only nonuniform modes can be excited and the plasma oscillations in the base crystal is strongly damped by the in-plane dissipation. The amplitude of plasma oscillations is small

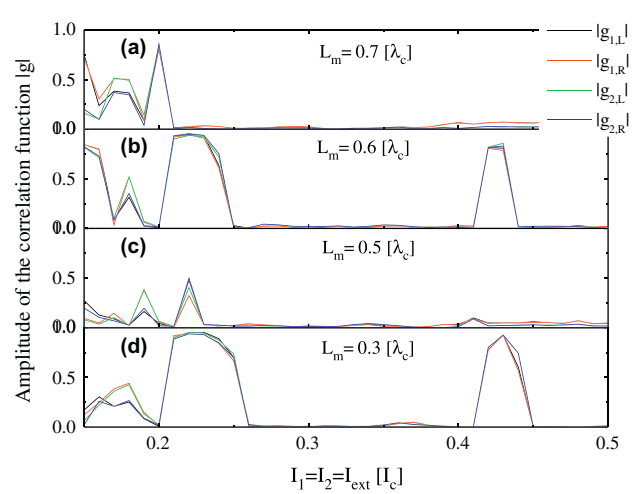

Fig. 5. Phase coherence of the Josephson oscillations between different stacks for different L_m. The coherence is measured by the correlations functions $|g_{j,L/R}|$ defined in Eq. (11).

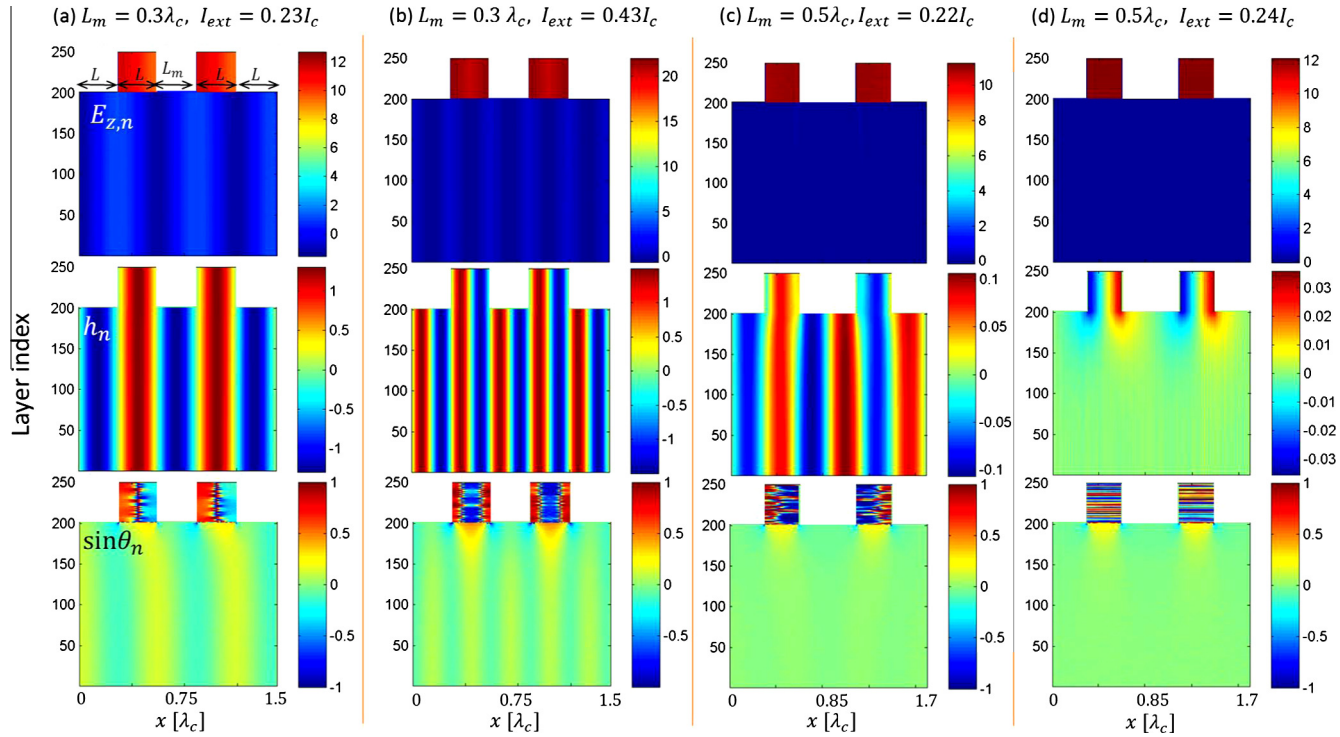

Fig. 6. Snapshots of the electric field (first row), magnetic field (second row) and Josephson current sin (θ_n) (third row) in the whole system. (a) and (b) are obtained at the first and second cavity resonance for $L_m = L$. (c) and (d) are results near the first cavity resonance for $L_m \neq nL$.

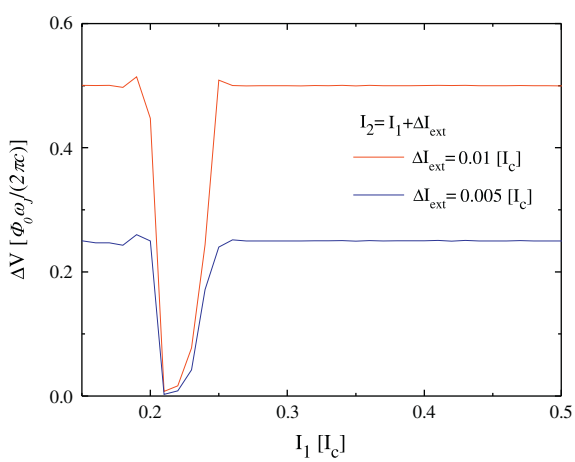

Fig. 7. Voltage difference between two mesas $\Delta V = V_2 - V_1$ when the mesas are biased by different current $I_2 = I_1 + \Delta I_{ext}$.

in comparison with the case $L_m = nL$, see Fig. 6c and d. Thus synchronization between the mesas is hard to attain. Therefore, the maximal synchronization is achieved when the position and size of mesas are commensurate with the standing wave in the base crystal, because the nonuniform plasma oscillations decay quickly in the base crystal.

Let us consider the phase shifts of Josephson oscillations between edges of mesas. As shown in Fig. 6a, the oscillating supercurrent changes sign from the left edge to the right edge in the same mesa. This indicates that the π phase kink is excited at the cavity resonance [34,35] which helps to pump energy into the plasma oscillations, as described by the term at the right-hand side of Eq. (3). As a consequence, the amplitude of the oscillations is enhanced sharply at the cavity resonances. In Fig. 6a and b, the Josephson oscillations at the left/right edges have the same phase for different stacks when $L_m = (2n + 1)L$. For $L_m = 2nL$, there is π phase shift between two mesas to match the standing wave in the base crystal.

In Fig. 7, we show the voltage difference between two mesas with $L_m = L$ when they are biased by different currents $I_2 = I_1 + \Delta I_{\text{lext}}$. At the cavity resonance when two mesas are synchronized, they have the same voltage despite that they are biased by slightly different currents. Away from the cavity resonance, two mesas decouple from each other and they oscillate at different frequencies.

5. Conclusions

We have investigated the synchronization of mesa array through the plasma oscillations in the base crystal. If one regards the mesa arrays and base crystal as a whole, the plasma oscillations inside depends on the configuration of mesa arrays as a result of geometrical resonance. The amplitude of the plasma oscillations and the tendency of synchronization is governed by the dissipation of the whole system, hence is determined by the configuration of mesa array. When the period of mesa array a close to the multiple integer of the mesa width L, $a \approx nL$, the dissipation is minimized and mesas are synchronized at cavity resonances of the whole system. Alternatively, one may treat mesa and base crystal separately. When the cavity resonance of mesa matches of that in the base crystal, mesa array is synchronized. Otherwise, the cavity resonance of the mesas is suppressed by the strong dissipation due to the radiation into the base crystal, and the mesa array is not synchronized. Therefore the optimal configuration for synchronization is $a \approx nL$. The above picture is corroborated by both analytical calculations and numerical simulations.

Acknowledgements

The authors thank T.M. Benseman, U. Welp, and L.N. Bulaevskii for helpful discussions. SZL gratefully acknowledges funding

support from the Office of Naval Research via the Applied Electrodynamics collaboration. AEK is supported by UChicago Argonne, LLC, operator of Argonne National Laboratory, a US DOE laboratory, operated under Contract No. DE-AC02-06CH11357.

References

[1] I.K. Yanson, V.M. Svistunov, I.M. Dmitrenko, Zh. Eksp. Teor. Fiz. 48 (1965) 976.
[2] A.H. Dayem, C.C. Grimes, Appl. Phys. Lett. 9 (1966) 47.
[3] Je. Zimmerma, J.A. Cowen, A.H. Silver, Appl. Phys. Lett. (10) (1966) 353.
[4] T.F. Finnegan, S. Wahlsten, Appl. Phys. Lett. 21 (1972) 541.
[5] A.K. Jain, K.K. Likharev, J.E. Lukens, J.E. Sauvageau, Phys. Rep. 109 (1984) 309.
[6] M. Darula, T. Doderer, S. Beuven, Supercond. Sci. Technol. 12 (1999) R1.
[7] P. Barbara, A.B. Cawthorne, S.V. Shitov, C.J. Lobb, Phys. Rev. Lett. 82 (1999) 1963.
[8] F. Song, F. Müller, R. Behr, A.M. Klushin, Appl. Phys. Lett. 95 (2009) 172501.
[9] R. Kleiner, F. Steinmeyer, G. Kunkel, P. Müller, Phys. Rev. Lett. 68 (1992) 2394.
[10] X. Hu, S.Z. Lin, Supercond. Sci. Technol. 23 (2010) 053001.
[11] S. Savel'ev, V.A. Yampol'skii, A.L. Rakhmanov, F. Nori, Rep. Prog. Phys. 73 (2010) 026501.
[12] I. Iguchi, K. Lee, E. Kume, T. Ishibashi, K. Sato, Phys. Rev. B 61 (2000) 689.
[13] I.E. Batov, X.Y. Jin, S.V. Shitov, Y. Koval, P. Müller, A.V. Ustinov, Appl. Phys. Lett. 88 (2006) 262504.
[14] M.H. Bae, H.J. Lee, J.H. Choi, Phys. Rev. Lett. 98 (2007) 027002.
[15] T.M. Benseman, A.E. Koshelev, K.E. Gray, W.-K. Kwok, U. Welp, K. Kadowaki, M. Tachiki, T. Yamamoto, Phys. Rev. B 84 (2011) 064523.
[16] M. Tachiki, T. Koyama, S. Takahashi, Phys. Rev. B 50 (1994) 7065.
[17] T. Koyama, M. Tachiki, Solid State Commun. 96 (1995) 367.
[18] M. Tachiki, M. Iizuka, K. Minami, S. Tejima, H. Nakamura, Phys. Rev. B 71 (2005) 134515.
[19] L.N. Bulaevskii, A.E. Koshelev, J. Supercond. Novel Magn. 19 (2006) 349.
[20] L.N. Bulaevskii, A.E. Koshelev, Phys. Rev. Lett. 99 (2007) 057002.
[21] S.Z. Lin, X. Hu, M. Tachiki, Phys. Rev. B77 (2008) 014507.
[22] A.E. Koshelev, L.N. Bulaevskii, Phys. Rev. B 77 (2008) 014530.
[23] M. Tachiki, S. Fukuya, T. Koyama, Phys. Rev. Lett. 102 (2009) 127002.
[24] T. Koyama, H. Matsumoto, M. Machida, K. Kadowaki, Phys. Rev. B 79 (2009) 104522.
[25] H. Asai, M. Tachiki, K. Kadowaki, Phys. Rev. B 85 (2012) 064521.
[26] S.Z. Lin, X. Hu, Phys. Rev. B 79 (2009) 104507.
[27] L. Ozyuzer, A.E. Koshelev, C. Kurter, N. Gopalsami, Q. Li, M. Tachiki, K. Kadowaki, T. Yamamoto, H. Minami, H. Yamaguchi, T. Tachiki, K.E. Gray, W.K. Kwok, U. Welp, Science 318 (2007) 1291.
[28] K. Kadowaki, H. Yamaguchi, K. Kawamata, T. Yamamoto, H. Minami, I. Kakeya, U. Welp, L. Ozyuzer, A. Koshelev, C. Kurter, K. Gray, W.-K. Kwok, Physca C 468 (2008) 634.
[29] H.B. Wang, S. Guénon, J. Yuan, A. Iishi, S. Arisawa, T. Hatano, T. Yamashita, D. Koelle, R. Kleiner, Phys. Rev. Lett. 102 (2009) 017006.
[30] H.B. Wang, S. Guénon, B. Gross, J. Yuan, Z.G. Jiang, Y.Y. Zhong, M. Grunzweig, A. Iishi, P.H. Wu, T. Hatano, D. Koelle, R. Kleiner, Phys. Rev. Lett. 105 (2010) 057002.
[31] M. Tsujimoto, K. Yamaki, K. Deguchi, T. Yamamoto, T. Kashiwagi, H. Minami, M. Tachiki, K. Kadowaki, R.A. Klemm, Phys. Rev. Lett. 105 (2010) 037005.
[32] M. Tsujimoto, T. Yamamoto, K. Delfanazari, R. Nakayama, T. Kitamura, M. Sawamura, T. Kashiwagi, H. Minami, M. Tachiki, K. Kadowaki, R.A. Klemm, Phys. Rev. Lett. 108 (2012) 107006.
[33] K. Yamaki, M. Tsujimoto, T. Yamamoto, A. Furukawa, T. Kashiwagi, H. Minami, K. Kadowaki, Opt. Express 19 (2011) 3193.
[34] S.Z. Lin, X. Hu, Phys. Rev. Lett. 100 (2008) 247006.
[35] A.E. Koshelev, Phys. Rev. B 78 (2008) 174509.
[36] S.Z. Lin, X. Hu, Phys. Rev. B 86 (2012) 054506.
[37] A.E. Koshelev, Phys. Rev. B 82 (2010) 174512.
[38] N. Orita, H. Minami, T. Koike, T. Yamamoto, K. Kadowaki, Physica C 470 (2010) S786.
[39] T.M. Benseman et. al., in preparation.
[40] A.E. Koshelev, L.N. Bulaevskii, J. Phys.: Conference Series 150 (2009) 052124.
[41] S. Sakai, P. Bodin, N.F. Pedersen, J. Appl. Phys. 73 (1993) 2411.
[42] L.N. Bulaevskii, M. Zamora, D. Baeriswyl, H. Beck, J.R. Clem, Phys. Rev. B 50 (1994) 12831.
[43] L.N. Bulaevskii, D. Domínguez, M.P. Maley, A.R. Bishop, B.I. Ivlev, Phys. Rev. B 53 (1996) 14601.
[44] M. Machida, T. Koyama, M. Tachiki, Phys. Rev. Lett. 83 (1999) 4618.
[45] A.E. Koshelev, I. Aranson, Phys. Rev. B 64 (2001) 174508.
[46] L.N. Bulaevskii, A.E. Koshelev, Phys. Rev. Lett. 97 (2006) 267001.